



SEISMIC BEHAVIOR OF MARMARA SUBMERGED TUNNEL: SSI, PSEUDO-THREE-DIMENSIONAL ANALYSES

A. Yoshino⁽¹⁾, C. Zulfikar⁽²⁾, J. Shimabuku⁽³⁾, M. Shoji⁽⁴⁾ and S. Tunc⁽⁵⁾

⁽¹⁾ Kozo Keikaku Engineering Inc., Tokyo, akari-yoshino@kke.co.jp

⁽²⁾ Civil Eng. Department, Engineering Faculty, Trakya University, Edirne, canzulfikar@trakya.edu.tr

⁽³⁾ Kozo Keikaku Engineering Inc., Tokyo, Japan, shimabuku@kke.co.jp

⁽⁴⁾ Kozo Keikaku Engineering Inc., Tokyo, Japan, shoji@kke.co.jp

⁽⁵⁾ Sentez Earth and Structure Engineering Inc., Istanbul, Turkey, stunc@syy.com.tr

Abstract

The Marmaray submerged tunnel is about 1400 m in length, running under the Bosphorus strait in Istanbul, Turkey. Since 2014 this tunnel has been monitored for seismic activities.

Due to the complicated geological characteristics where the tunnel is located and large scale of analysis domain, considering the soil structure interaction (SSI) effects becomes important. This paper discusses the characteristics of earthquake wave propagation in the tunnel. The local site effects have been investigated analytically using the SuperFLUSH/2D program [1]. This program can perform a pseudo-three-dimensional analyses considering equivalent stiffness for the in-plane and out-of-plane directions. Due to large-scale of the tunnel, a domain of around 5km length is considered for the FEM model. The tunnel and soil are modelled by beam and plane strain elements respectively. Input seismic waves in the in-plane and out-of-plane directions are considered.

The previous studies [2], [3] clarified the importance of SSI effects using two-dimensional (in-plane direction) model. In this study, a pseudo-three-dimensional analysis is performed, by considering the soil stiffness and the input motion angle of incidence as study parameters. Good correlation between the analysis results and observed data at the sedimentary layer, but there were results deviated near the bedrock. This can be attributed to the presence of irregular topography in orthogonal N-S direction, which cannot be considered in the out-of-plane direction of pseudo-three-dimensional analysis model.

Keywords: Tunnel, SSI, Monitoring System, Simulation Analysis

1. Introduction

Previous studies [2], [3] using a two-dimensional model shows that while analysing a submerged tunnel, considering the soil structure interaction (SSI) effects become important, especially due to the complicated geological characteristics at the tunnel's location and the large scale of analysis domain. This paper investigates the SSI effects in the two orthogonal directions (EW, NS) through a pseudo-three dimensional analysis.

2. Analytic Method

In the present study, the SuperFLUSH/2D program[1] is used for analysis. This program can perform a pseudo-three-dimensional analyses; a 2-D analysis considering an equivalent stiffness in the in-plane and out-of-plane directions. Fig.1 shows the considered 3D-stresses and Eq. (1) and Eq. (2) are the constitutive stress-strain equations in the in-plane and out-of-plane directions respectively.

The large shear deformations which occur in soils during strong earthquakes introduces non-linear effects in the soil. The program takes these nonlinear effects into account by the introduction of an equivalent linear method. It analyzes response in the frequency domain using a complex stiffness as shown in Fig. 2. Fig. 3 shows the strain-dependent curve, where strain is calculated from three-dimensional field (in-plane and out-of-plane strains).

Because a FEM model is used, it is necessary to simulate the semi-infinite soil at boundaries. Two types of boundaries are available in SuperFLUSH/2D; the viscous dashpot boundary and the energy transmitting boundary. Fig. 4 shows the boundary condition for the pseudo-three-dimensional models. In the out-of-plane direction, the semi-infinite soil is modelled by the FEM model which does not consider the influences due to the presence of the tunnel structure.

$$\begin{Bmatrix} \sigma_x \\ \sigma_z \\ \tau_{xz} \end{Bmatrix} = \begin{bmatrix} \frac{E(1-\nu)}{(1+\nu)(1-2\nu)} & \frac{E\nu}{(1+\nu)(1-2\nu)} \\ \frac{E\nu}{(1+\nu)(1-2\nu)} & \frac{E(1-\nu)}{(1+\nu)(1-2\nu)} \end{bmatrix} G \begin{Bmatrix} \varepsilon_x \\ \varepsilon_z \\ \gamma_{xz} \end{Bmatrix} \quad (1)$$

$$\begin{Bmatrix} \tau_{xy} \\ \tau_{yz} \end{Bmatrix} = \begin{bmatrix} G & \\ & G \end{bmatrix} \begin{Bmatrix} \gamma_{xy} \\ \gamma_{yz} \end{Bmatrix} \quad (2)$$

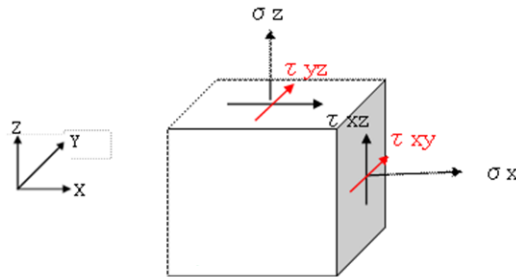


Fig. 1 – 3D-stress

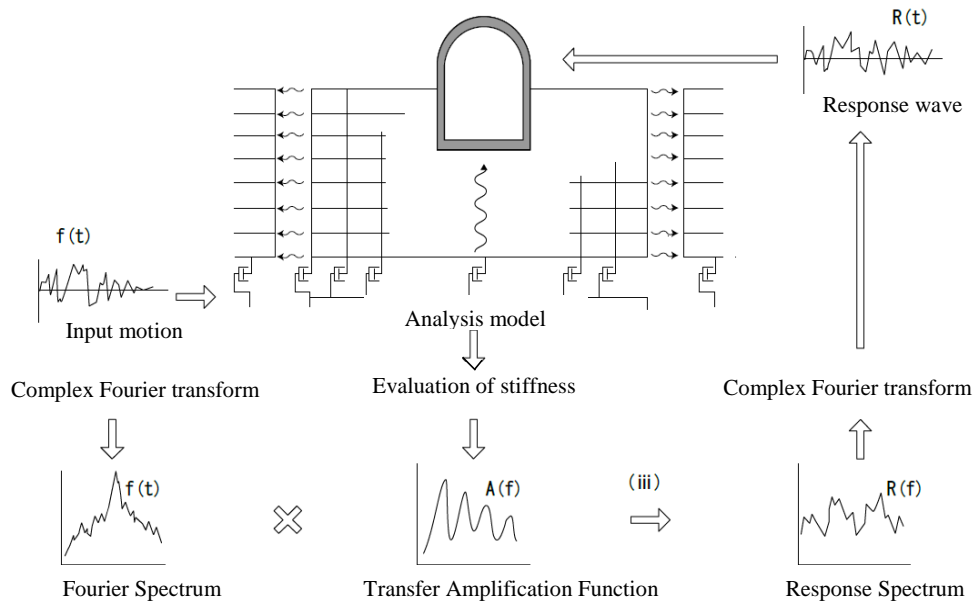


Fig. 2 – Frequency response analysis

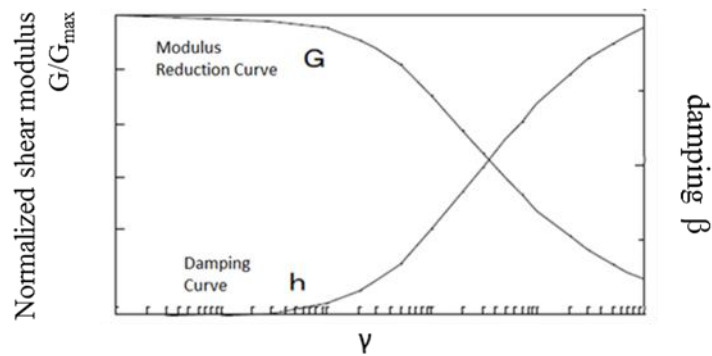


Fig. 3 – Strain-dependent curve

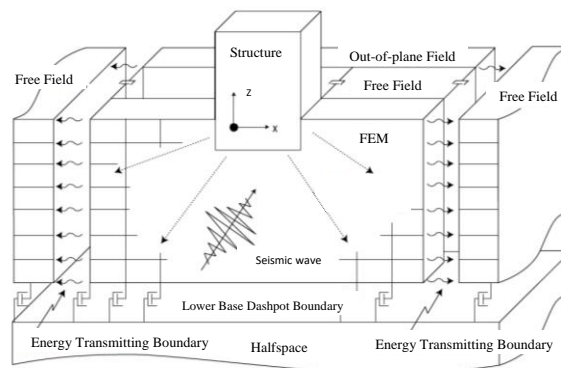


Fig. 4 – Boundary conditions for analysis model

3. Seismic Monitoring

3.1 Monitoring Points

The Marmaray tube tunnel was formed from 13 concrete segments. 11 of them were immersed under the sea and two are located at each side of the strait. The observed data used for comparison with the analysis results, were measured at the segments present inside the undersea tunnel shown in Fig. 5. Two tri-axial sensors were positioned at evenly spaced intervals in each segment of the undersea tunnel to monitor the seismic waves. Twenty-six sensors in total were used. Fig. 6 shows the monitoring system.

3.2 Observed Records

The present study analyzed the observed waves traveling in the direction of the tunnel (EW direction) that occurred during the earthquake at Black Sea coast, M3.8 May 2, 2014[2]. Additionally this study analyzed the observed waves traveling in the orthogonal direction of the tunnel (NS direction). Fig. 7 shows the observed acceleration records at monitoring points A1, A4, A6, A8, A10 and A12 (6 of the 13 monitoring points in the tunnel) and Fig. 8 shows the acceleration response spectra at the aforementioned observation points normalized with respect to point A0, which is located at the bedrock. The amplitude of the observed acceleration records in NS direction were higher than the ones in EW direction especially in sedimentary layers.

Fig. 8 shows that the acceleration response spectra of point A1 and A12 are similar to that of A0 because A1 and A12 are located near the bedrock. On the other hand, in the case of A6 and A7, the effects of the sedimentary layer are clearly visible on Acceleration Response Spectra with a peak at around 1.0 sec, which corresponds to the fundamental period of the site and also corresponds to the value calculated analytically.

4. Analysis Conditions

4.1 Analysis Model

The analysis model was 5,400 m wide and 250 m in depth, and considers the tunnel, which is at a depth of 55 m. The soil was modeled using plane strain elements, and the tunnel was modeled using beam elements. Since majority of the response obtained from Fourier analysis is within 20Hz, the maximum analysis frequency was set at 20Hz. Moreover, since input wave used in analyses is small, linear analyses were conducted.

Fig. 9 shows the complete analysis model, an expanded view of the Bosphorus Strait section of the model, and a part of the meshed model. In the case of the out-of-plane analysis model, similar soil characteristics as the FEM model were assumed in the orthogonal direction. The observed records were deconvoluted to assign the input seismic motion at the bottom of the model.

Table 1 and Table 2 show soil and tunnel properties. Tunnel properties were calculated from a typical section of the tunnel[4].

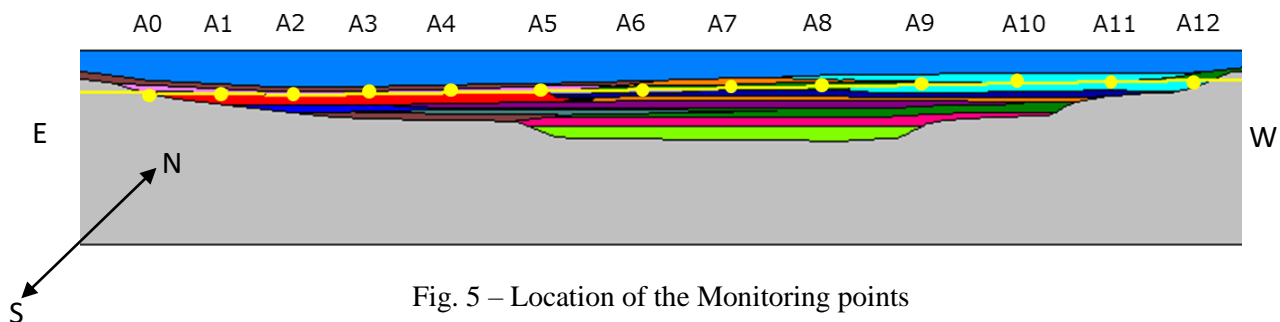


Fig. 5 – Location of the Monitoring points

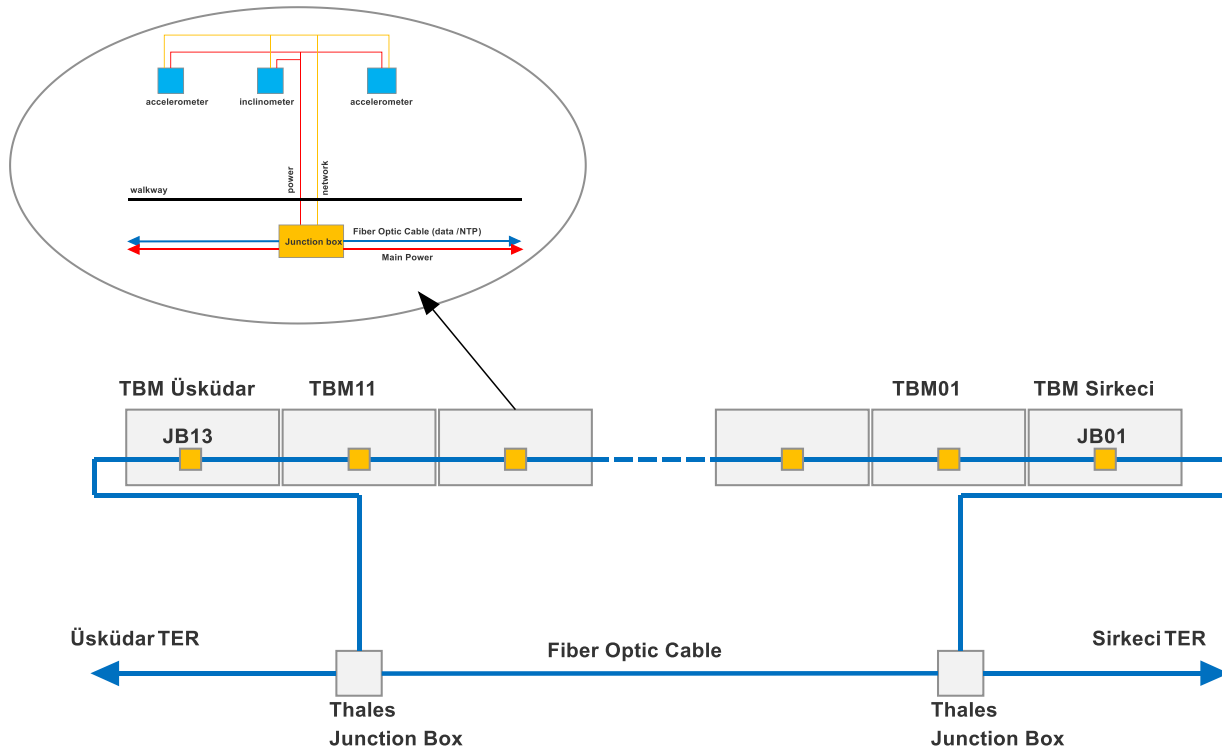


Fig. 6 – Earthquake monitoring system of the Marmaray submerged Tube Tunnel

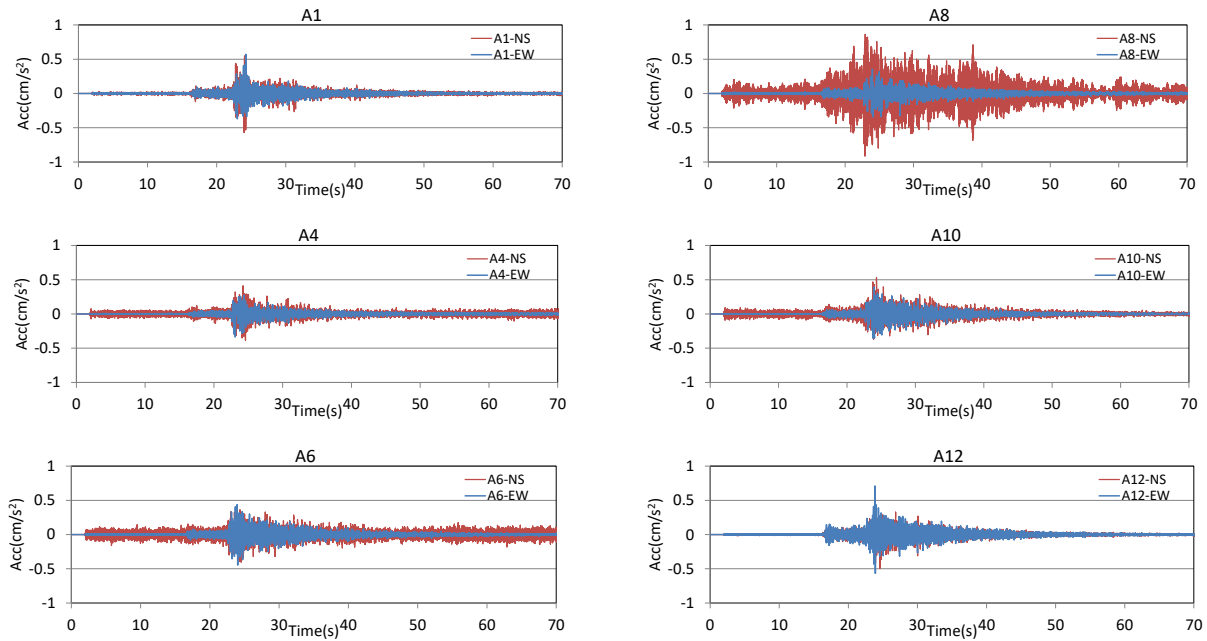


Fig. 7 – Observed horizontal acceleration record

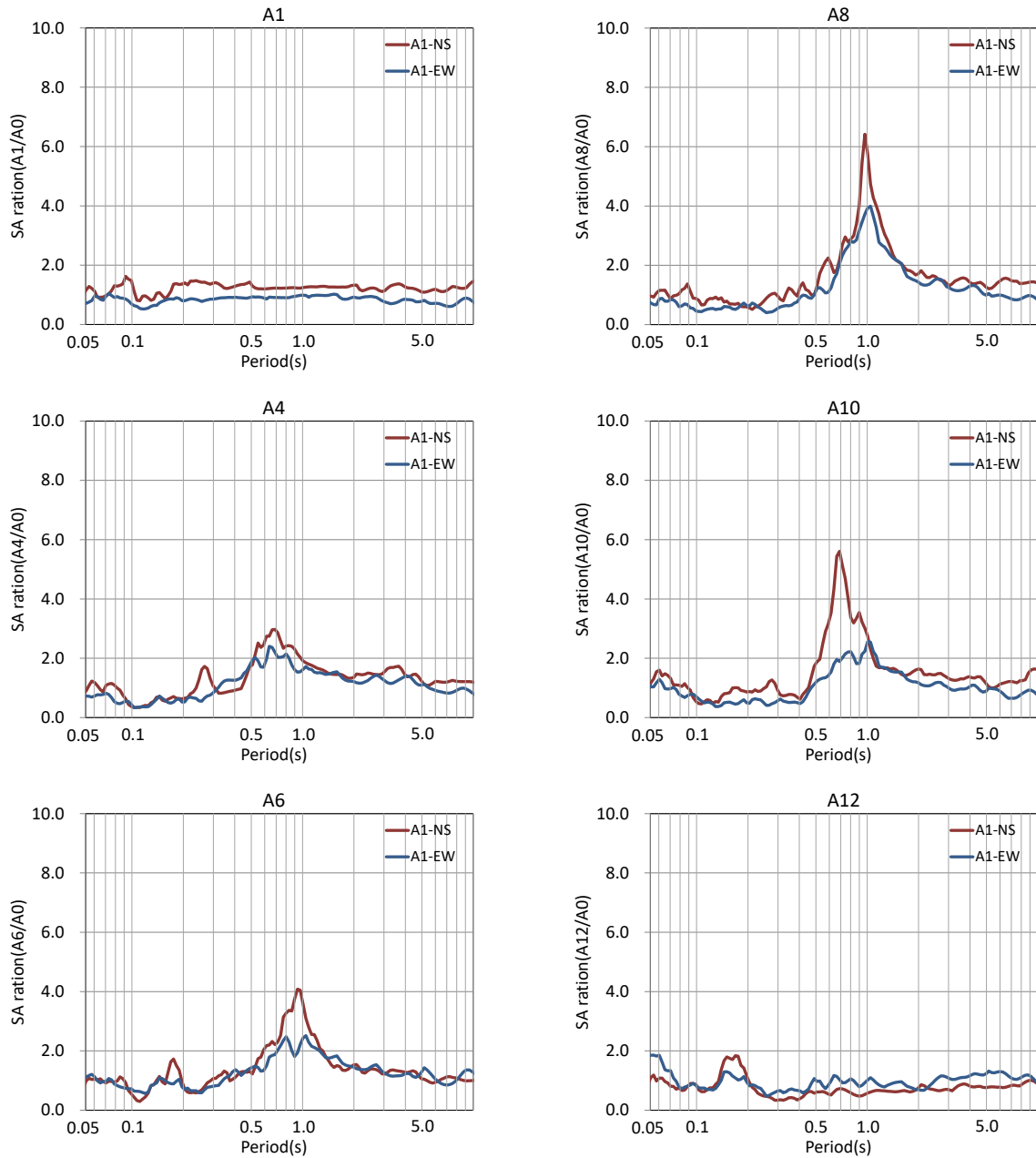


Fig. 8 – Normalized acceleration response spectra (damping 5%)

4.2 Analysis Cases

Table 3 shows the various cases considered for analysis. To correspond with the previous study, [3], the case comprising of 70% of original soil stiffness and inclined wave input (angle of incidence 25%) are considered.

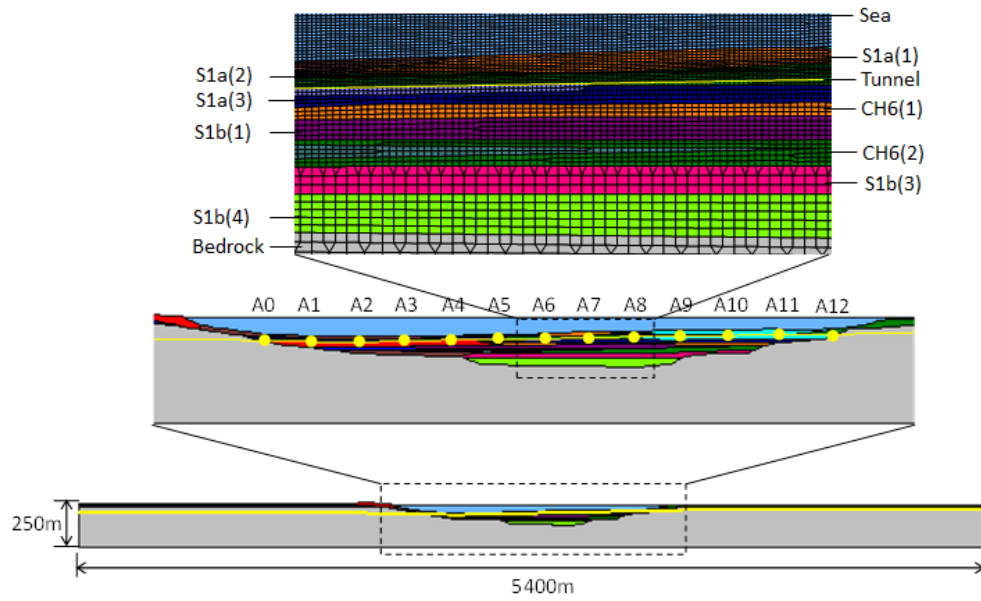


Fig. 9 – Model of Analysis (EW direction)

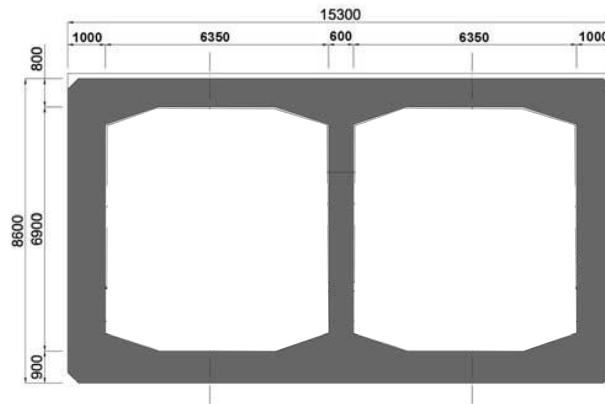


Fig. 10 – Geometrical properties of the tube tunnel [4]

Table 1 – Soil properties

Soil	Unit weight γ (kN/m ³)	Shear modulus G (kN/m ²)	Damping h (%)	
Sedimentary layers	F	17.7	4.52E+05	5
	SW	18.2	7.11E+05	5
	S1	17.5	4.02E+04	5
	S1a	18.5	7.55E+04 ~ 1.18E+05	5
	S1b	17.5 ~ 19.0	1.40E+05 ~ 2.75E+05	5
	CH4	17.0	3.90E+04	5
	CH5	17.0 ~ 17.5	6.93E+04 ~ 1.83E+05	5
	CH6	17.5	7.14E+04 ~ 1.83E+05	5
	S2	17.0	6.70E+04	5
Bedrock	22.8	5.55E+06	1	



Table 2 – Property for tunnel [4]

Unit weight γ (kN/m ³)	Young's modulus ¹⁾ E (kN/m ²)	Poisson's ratio ν	Moment of inertia I (m ⁴)	Area A (m ²)	Damping h (%)
24.5	3.1E+07	0.20	488.3	46.31	5

1) Calculated considering $f_c=40$ N/mm² in accordance to the Japanese code for RC structures

Table 3 – Analysis cases for this study

	Shear Modulus in sedimentary layers	Shear Modulus in sedimentary layers	Angle of incidence (θ)
Case1	Does Not Exist	Same as Table 1	0°
Case2	Exists	Same as Table 1	0°
Case3			25°
Case4		70% of Table 1	0°
Case5			25°

5. Results of Analysis

The analysis of the observed records and wave propagation analysis on the tunnel structure with local site effects have been discussed. Fig. 5 shows that monitoring points A1 and A12 points are located close to bedrock, A6 and A8 points are located at the center of the tunnel where the sedimentary layers are considerable. The comparisons between the acceleration response spectra of the observed records and the analysis results for different cases has been performed, through the transfer function, which has been normalized with respect to A0, as shown in Fig. 11 to Fig. 14. Fig. 11 and Fig. 12 show the results for in-plane analyses, Fig. 13 and Fig. 14 show the results for out-of-plane analyses.

Fig. 11 shows that the peak of Case1, where the effects of the tunnel structure are not considered, is different from the other cases, where the structural effects of the tunnel are considered. Fig. 12 shows that the except for point A8, Case1 gives higher response than the other cases. This can be attributed to the fact that the soil is restrained by the tunnel structure and the vibration characteristics of Case1 is different from the other cases. By contrast, Fig. 13 and Fig. 14 show that the results of Case1 are similar to the results of the other cases, which show that soil behaviour is predominantly in this direction, and the effects of the tunnel is comparatively negligible

Comparing the in-plane analyses to out-of-plane analyses results, a different tendency is observed near the bedrock. Fig. 13 shows that the results for analyses are close to observation results at the monitoring points of A6 and A8. On the other hand, at the points of A1 and A12 near the bedrock, analysis results deviated from the observation results. One reason could be due to the lack of consideration of the irregular topography in out-of-plane direction, in analysis model. Though the analysis model assumes that the ground model in Fig. 9 infinitely continuous in out-of-plane direction, the actual soil topography is complex and the sedimentary layer is not infinite in the out-of-plane direction. This causes the observation results to be smaller than analysis results.

As for soil stiffness and angle of incidence, though Case5 (soil stiffness 70%, angle of incidence 25%) was closer to observation results in the in-plane analysis, Case3 (soil stiffness 100%, angle of incidence 25%) was closer to observation results in the case of out-of-plane analysis. Therefore it is consider that soil properties should be carefully chosen during pseudo-three-dimensional analyses. Fig. 14 also shows the analysis results are higher than observation results near to bedrock. The above result shows the necessity to consider the out-of-plan soil e complexity or the need to perform a three dimensional analyses.

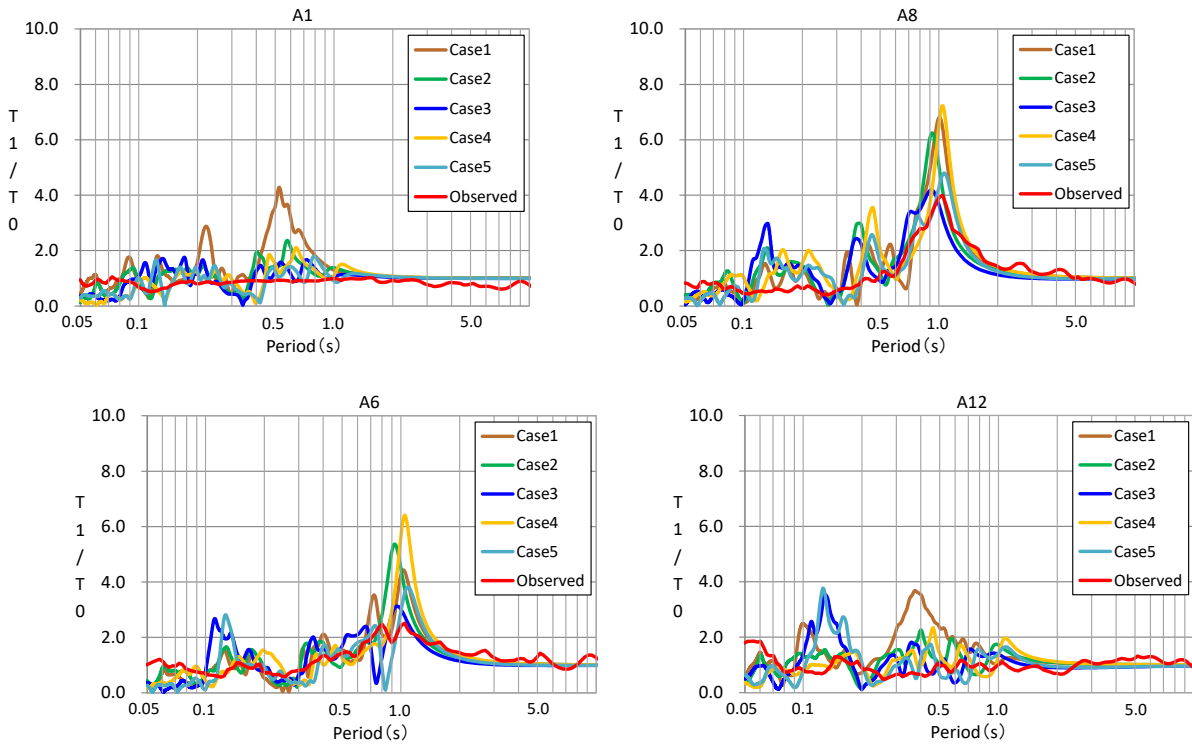


Fig. 11 – Transfer functions normalized with respect to A0 (in-plane)

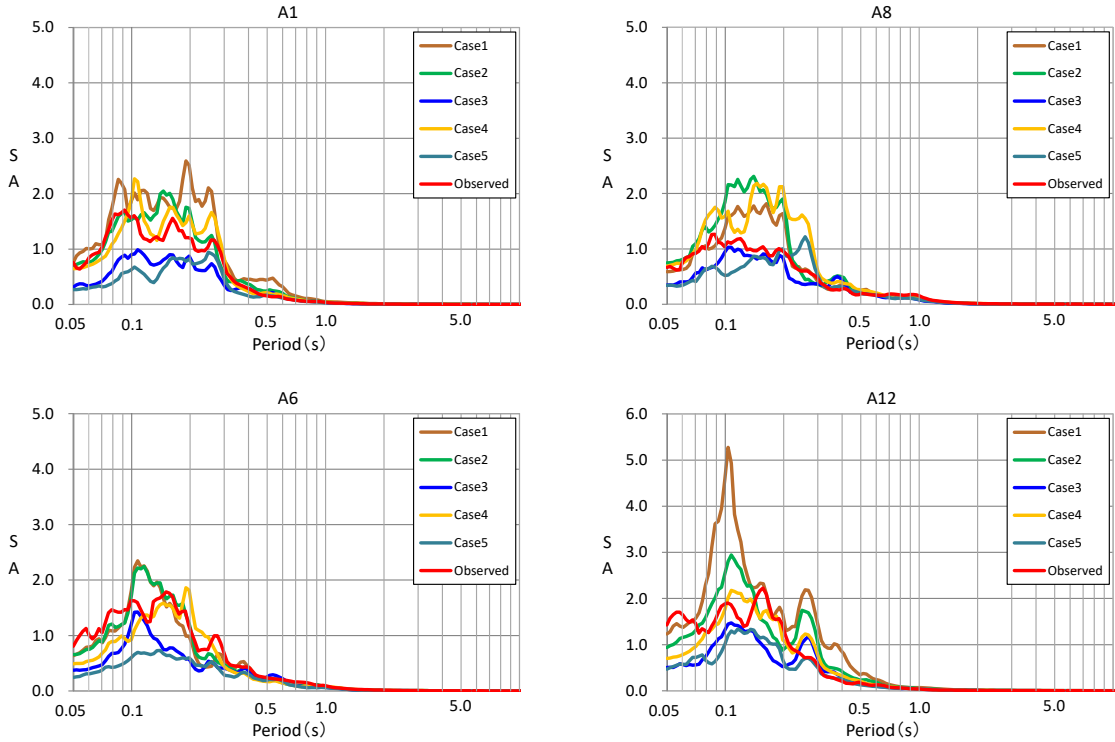


Fig. 12 – Acceleration response spectra (in-plane)

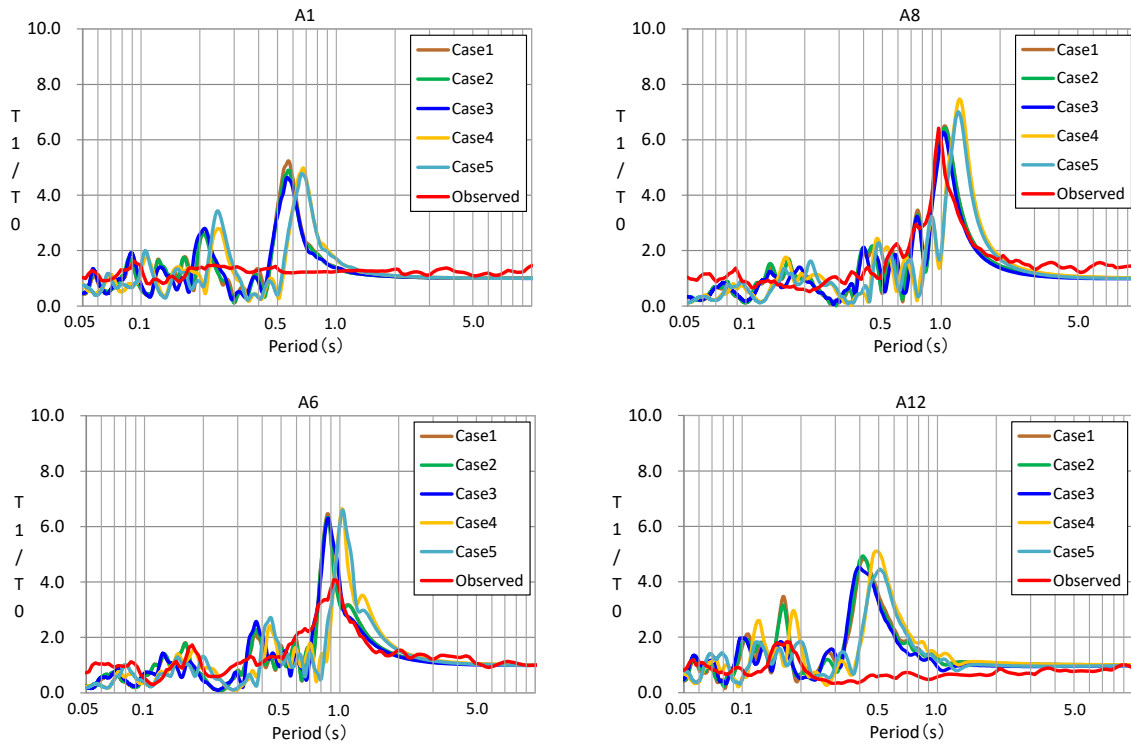


Fig. 13 – Transfer functions normalized with respect to A0 (out-of-plane)

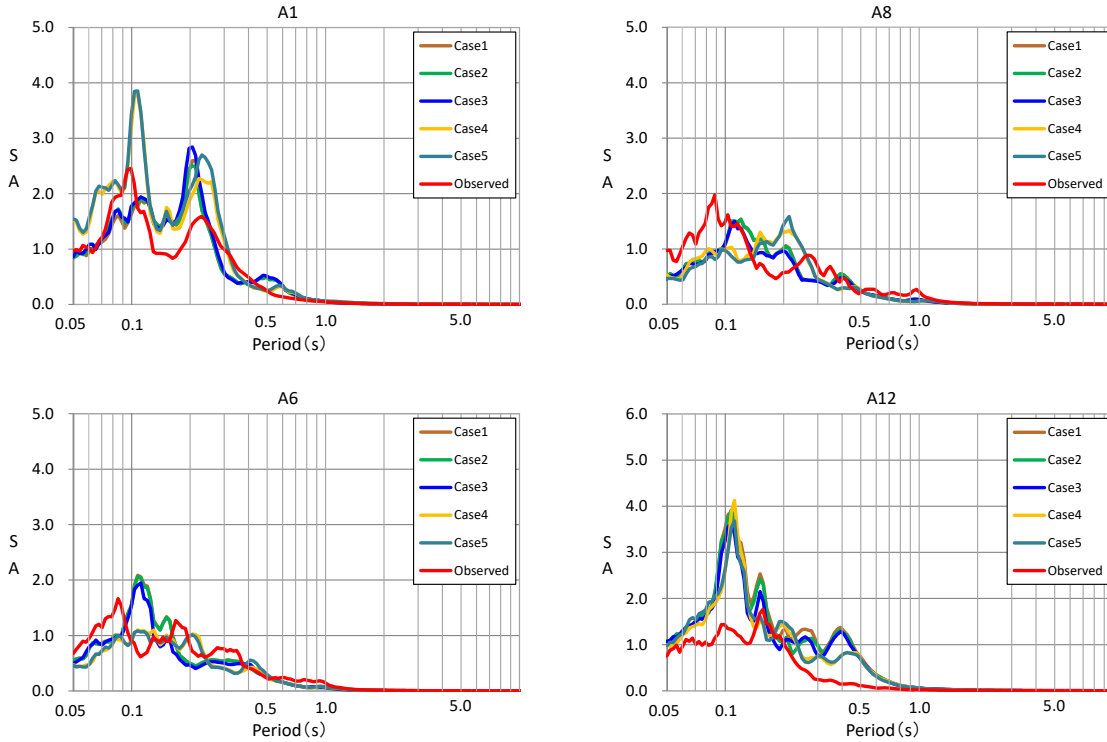


Fig. 14 – Acceleration response spectra (out-of-plane)

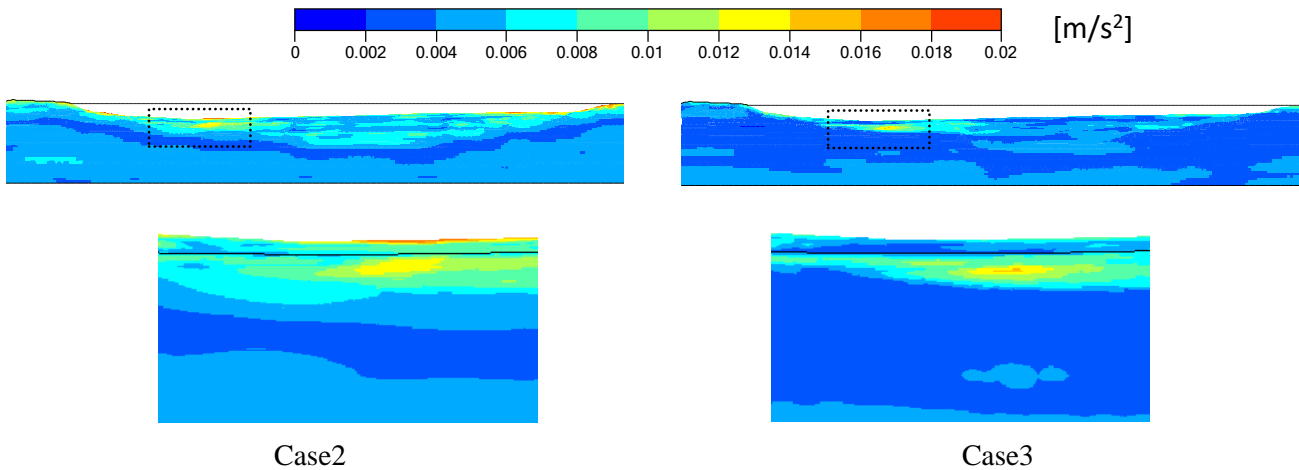


Fig. 15 – Maximum horizontal acceleration contour (in-plane)

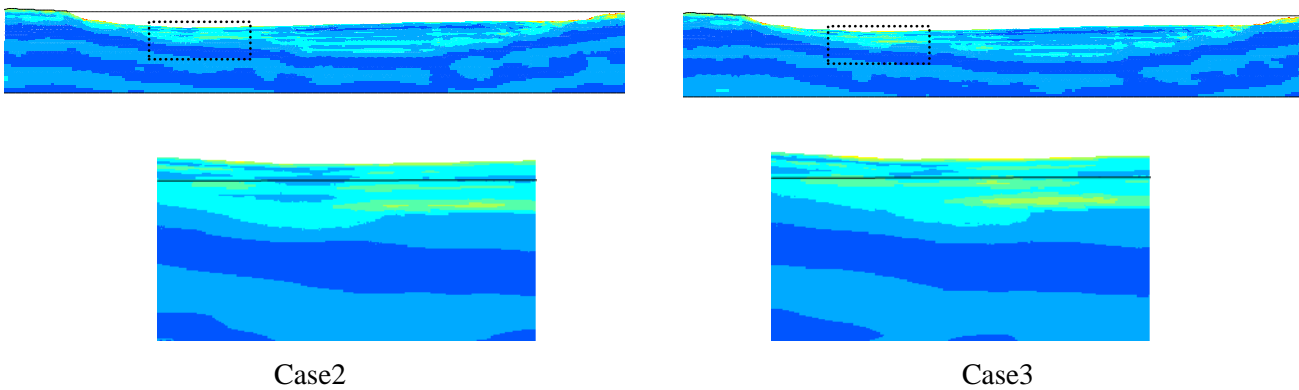


Fig. 16 – Maximum horizontal acceleration contour (out-of-plane)

Fig. 15 and Fig. 16 show the maximum horizontal acceleration contour for in-plane and out-of-plane analysis. Fig. 15 shows that the distribution of acceleration is different among Case2 and Case3 due the reflection of propagating seismic waves. In Fig. 16, the acceleration distribution of Case2 is almost the same as Case3. These results are caused due to the topographical characteristics of the soil. Though a complex topography can be modeled in EW direction, it cannot be modeled in NS direction, due to the limitations of the analysis method.

6. Conclusion

A ground response analysis considering the SSI effect has been conducted for a submerged tube tunnel crossing the Marmaray, by comparing the analysis results with observation records during past earthquake events.

The results of this study lead to the following conclusions:

- Analyses results clarified the importance of considering the SSI effect especially in the longitudinal direction of the structure.
- Analyses results correlate to the observation results where soil topography comparatively continues in out-of-plane direction.



7. References

- [1] Kozo Keikaku Engineering Inc and Jishin Kougaku Kenkyusyo Inc. “SuperFLUSH/2D ver6.0 manual”.
- [2] A. Yoshino, C. Zulfikar, S. Tunc, J. Shimabuku, M. Shoji, (2015): SEISMIC RESPONSE OF MARMARAY SUBMERGED TUNNEL CONSIDERING SOIL-STRUCTURE INTERACTION. *3rd Turkish Conference on Earthquake Engineering and Seismology 2015/10*, Izmir, Turkey.
- [3] C. Zulfikar, A. Yoshino, Y. Mitsuhashi, M. Shoji, (2015): SEISMIC BEHAVIOR OF MARMARAY SUBMERGED TUBE TUNNEL CONSIDERING SOIL-STRUCTURE INTERACTION. *8th National Conference on Earthquake Engineering 2015/11-14 May*, Istanbul, Turkey.
- [4] Fumiko K, Atsushi H, Michitaka M, (2008): Turkey Bosphorus Crossing Tunnel Construction. *Journal of Construction (in Japanese)2008/06*, 65-71.